Biomedicine & Pharmacotherapy 66 (2012) 464–468

Available online at
SciVerse ScienceDirect
www.sciencedirect.com

Elsevier Masson France
EM|consulte
www.em-consulte.com/en

Original article

Fibronectin expression is decreased in metastatic renal cell carcinoma following endostatin gene therapy

Karen Cristina Barbosa Chaves [a], Lauro Thiago Turaça [b], João Bosco Pesquero [b], Gregory Mennecier [c], Maria Lucia Zaidan Dagli [c], Roger Chammas [d], Nestor Schor [a], Maria Helena Bellini [a,*,e]

[a] Nephrology Division, Medicine Department, Federal University of Sao Paulo, Sao Paulo, Brazil
[b] Biophysics Department, Federal University of Sao Paulo, Brazil
[c] Department of Pathology, University of Sao Paulo, School of Veterinary Medicine and Animal Science, Sao Paulo, Brazil
[d] Department of Radiology, University of Sao Paulo, Sao Paulo, Brazil
[e] Biotechnology Department, IPEN-CNEN, University of Sao Paulo, Sao Paulo, Brazil

ARTICLE INFO

Article history:
Received 29 February 2012
Accepted 15 April 2012

Keywords:
RCC
Endostatin
Orthotopic metastatic model
Fibronectin

ABSTRACT

Tumor cells induce the disruption of homeostasis between cellular and extracellular compartments to favor tumor progression. The expression of fibronectin (FN), a matrix glycoprotein, is increased in several carcinoma cell types, including renal cell carcinoma (RCC). RCC are highly vascularized tumors and are often amenable to antiangiogenic therapy. Endostatin (ES) is a fragment of collagen XVIII that possesses antiangiogenic activity. In this study, we examined the modulation of FN gene expression by ES gene therapy in a murine metastatic renal cell carcinoma (mRCC) model. Balb/C mice bearing Renca cells were treated with NIH/3T3-LXSN cells or NIH/3T3-LendSN cells. At the end of the experiment, the ES serum levels were measured, and the FN gene expression was assessed using real-time PCR. The tissue FN was evaluated by western blotting and by immunofluorescence analysis. The ES serum levels in treated mice were higher than those in the control group ($P < 0.05$). ES treatment led to significant decreases at the FN mRNA ($P < 0.001$) and protein levels ($P < 0.01$). Here, we demonstrate the ES antitumor effect that is mediated by down-regulation of FN expression in mRCC.

1. Introduction

Renal cell carcinoma (RCC) is the 13th most common cancer worldwide and accounts for 4% of all adult malignancies in the USA [1]. Approximately 25 to 30% of patients with RCC have distant metastases at diagnosis, and another 33% develop systemic recurrence after primary tumor resection [2].

In sporadic (noninherited) RCC, von Hippel-Lindau gene (VHL) alteration is a common event. VHL is a tumor suppressor that is inactivated either by a loss of heterozygosity or by epigenetic alterations [3]. VHL gene inactivation leads to HIF-1α stabilization and the consequent induction of genes such as vascular endothelial growth factor (VEGF) and platelet-derived growth factor (PDGF), which are responsible for tumor-associated angiogenesis [4,5].

In the case of localized disease, RCC is curable with surgery, but for patients with distant metastases, the prognosis is poor [6]. The treatment of metastatic renal cell cancer (mRCC) has advanced significantly with a better understanding of the disease pathogenesis. Recently, some multitarget-oriented drugs have shown impressive activity in mRCC, with a high percentage of patients exhibiting a partial response and/or disease stabilization; additionally, these drugs have had a significant impact on survival [7–10].

Integrins are involved in the pathogenesis and progression of many diseases, including malignant tumors. Integrins directly bind components of the extracellular matrix (ECM) and provide the traction necessary for cell motility and invasion. The interaction between integrins and the ECM is essential for endothelial cell proliferation and angiogenesis. Integrin $\alpha_5\beta_1$ has been identified as one of the integrins involved in these processes [11,12].

Integrin $\alpha_5\beta_1$ is a receptor of fibronectin (FN), a fibrillar glycoprotein that is a well-characterized ECM protein [13]. FN exists in two forms, termed cellular FN (cFN) and plasma FN (pFN). pFN is produced in the liver, and cFN is produced by fibroblasts and many other cell types, including tumor cells [14]. FN is deposited as a polymerized insoluble matrix by endothelial cells to provide support and facilitate cell migration and adhesion during angiogenesis [15]. FN deposition requires intact focal adhesions, which in turn serve as anchors for the actin stress fibers involved in cell locomotion [15].

In RCC, FN appears to promote cell migration and invasion [16,17]. Additionally, in the metastatic stage of the disease, cFN

* Corresponding author.
E-mail address: mhmarumo@terra.com.br (M.H. Bellini).

0753-3322/$ – see front matter © 2012 Elsevier Masson SAS. All rights reserved.
http://dx.doi.org/10.1016/j.biopha.2012.04.003

levels are significantly increased, suggesting a possible role for cFN in advanced RCC [13].

Endostatin (ES), which is derived from the noncollagenous (NC1) domain of the α1 chain of type XVIII collagen, is a potent endothelial cell-specific inhibitor of angiogenesis and tumor growth in mice [18–22]. At present, the exact molecular mechanism of action of ES is not completely elucidated. ES has been shown to bind to integrin $\alpha_5\beta_1$, the major FN receptor in endothelial cells, on the surface of proliferating endotheliocytes [23,24]. Wickstrom and collaborators showed that ES treatment induces disassembly of the focal adhesions and actin stress fibers and disturbs the deposition of the FN matrix [25].

In previous reports by our group, subcutaneous injections of ES-transduced cells resulted in significant antitumor effects in a murine model of mRCC. A histological analysis of treated tumors showed decreased microvascular density and reduction of the nodule number and area as well as decreased proliferation of the tumor cells, which was associated with leukocyte infiltration [21,22]. In this study, we evaluated the expression of FN in metastatic lung tissue after retroviral ES therapy.

2. Materials and methods

2.1. Cell Lines

The NIH/3T3-LendSN-clone 3 was utilized for endostatin expression, and NIH/3T3-LXSN was used as a control, as previously described [19]. Both cell lines were maintained in DMEM medium (Life Technologies Corporation®, Grand Island, NY, USA) with high glucose content (4.5 g/l at 25 mM) and were supplemented with 100 U/ml penicillin, 100 μg/ml streptomycin, and 10% fetal bovine serum.

The murine kidney carcinoma cell line, Renca (Cell Lines Service®, Germany), was obtained from a murine transplantable renal adenocarcinoma of spontaneous origin. The cells were maintained in RPMI 1640 medium (Life Technologies Corporation®, Grand Island, NY, USA) that was supplemented with 10% fetal bovine serum, 2 mM L-glutamine, 1 mM sodium pyruvate, 1% minimal Eagle's medium nonessential amino acids, 100 U/ml penicillin and 100 μg/ml streptomycin (Gibco®, Grand Island, NY, USA).

All of the cell lines were maintained in a humidified chamber at 37 °C with 5% carbon dioxide.

2.2. Animals

Male Balb/C mice, 10–12 weeks old, were obtained from the Animal Facility of IPEN/CNEN-SP, Sao Paulo, Brazil. All of the animals were cared for in accordance with the standards of the Institute under a protocol that was approved by the Animal Experimentation Ethics Committee (Number of Process: 87/11).

2.3. Orthotopic RCC tumor model

The mice were anesthetized by intraperitoneal injection with ketamine (100 mg/kg body weight, Ketalar®; Parke-Davis, Morris Plains, NJ, USA) and xylazine (10 mg/kg body weight, Phoenix Scientific, Inc.®, St. Joseph, MO, USA). The left kidney was exposed through a left-flank incision and 2×10^5 Renca cells that were suspended in 10 μl of phosphate-buffered saline (PBS) with the aid of a glass syringe (Hamilton Company® Reno, NV, USA) were inoculated into the renal subcapsular space. The kidney was then returned to the body cavity, and the muscle and skin were sutured using surgical clips.

The left kidney was removed by unilateral nephrectomy 7 days after Renca cell inoculation. The mice were divided into two experimental groups with $n = 10$ each: a control group and an ES-treated group. The groups received a subcutaneous injection of $3{,}6 \times 10^6$ NIH/3T3-LXSN or the NIH/3T3-LendSN-clone 3 cells (ES production levels = 1.36 μg/ml), respectively.

2.4. Plasma ES levels determination

At the end of the experiment the blood samples of mice were taken into test tubes with EDTA, plasma components separated and then frozen at −20 °C. Samples were thawed at the time of study and plasma ES levels were measured using a murine ES enzyme immunoassay kit (USCN Life Science & Technology Company, Wuhan, China), in accordance with the manufacturer instructions. The ES concentrations were determined at least in duplicate, and the assay reproducibility was confirmed. ELISA plates were read using the Multiskan EX Microplate Reader (Labsystems, Milford, MA, USA).

2.5. Protein extraction and Western blotting

The lungs (100 mg wet wt) were homogenized in 2 ml of extraction buffer (0.1 M Tris, 0.01 M EDTA, 1% SDS and 0.01 M DTT at pH 8.0). After centrifugation at 3000 rpm for 10 min, the supernatant was collected and stored at −20 °C. The protein concentration was determined using the *DC* Protein Assay Kit I (Bio-Rad Laboratories, Hercules, CA, USA) according to the manufacturer's instructions. SDS-polyacrylamide gel electrophoresis was conducted under reducing conditions. The 5% and 12% separating gels were overlaid with a stacking gel containing 4% polyacrylamide. Samples with the same protein concentration (50 μg per lane) were separated at 100 V/plate for approximately 1.5 h until the dye front reached the end of the gel. After electrophoresis, the gels were transferred onto nitrocellulose membranes at 50 V for 50 min. Following the transfer of proteins, the blotted membranes were blocked with 5% nonfat dry milk for 1 h and incubated with primary antibodies for Fibronectin (EP5) (sc-8422, Santa Cruz Biotechnologies®, Inc., California, USA, 1:200) and GAPDH (Cat. #MAB374, Chemicon, Temecula®, CA, USA, 1:500) overnight, and the blots were developed using goat anti-mouse IgG biotinylated secondary antibody (AP308P, Millipore®, Temecula, CA, USA, 1:5000) for 1 h. The bands were visualized using enhanced chemiluminescence (ECL system; Amersham Bioscience®, Piscataway, NJ, USA) in accordance with the manufacturer's guidelines. The Western blot signal was normalized to the GAPDH band density. To quantify the bands obtained by Western blotting, we performed an ImageJ software-based analysis (http://rsb.info.nih.gov/ij/).

2.6. Immunofluorescence analysis

At the end of the experiment, the animals were sacrificed following the guidelines for euthanasia of the American Veterinarian Medical Association. The metastatic lungs were excised, washed in PBS, fixed in PBS-buffered 3.7% formalin for 24 h and then routinely processed for paraffin embedding. A histological analysis was performed on 4 μm sections that were stained with hematoxylin and eosin.

The metastatic lungs sections were freshly cut and hydrated, and a heat-induced epitope retrieval was performed by immersing the slides in citrate buffer (0.1 ml/l, pH 6.0) and incubating them in a microwave oven for 15 min. A solution of 5% BSA and 0.1% Triton X-100 (Sigma-Aldrich) in PBS for 30 min was used to block non-specific reactions, and then, the slides were incubated with a primary mouse monoclonal antibody to Fibronectin (O.N.297, Santa Cruz, CA, USA, 1:50) overnight in a humidified chamber at

4 °C. After washing, a secondary antibody, anti-mouse Alexa Fluor® 488 (Invitrogen Corporation, Eugene, OR, 1:100), was used to detect the primary antibody, and the slides were incubated for 2 h. After several PBS washes, each section was counterstained using a premixed solution of 4,6-diamidino-2-phenylindole (DAPI) and antifade mounting media (ProLong Gold antifade reagent with DAPI; Invitrogen Corporation, Eugene, OR®). The fluorescence signals were observed under a fluorescence Nikon E-800 microscope (Tokyo, Japan), and the images were obtained with a DXM1200F digital camera (Nikon Instruments Inc., Melville, NY, USA) and analyzed using the EclipseNet® software for Nikon cameras.

2.7. RNA extraction

Metastatic lung tissue (100 mg) was homogenized on a rotor-stator Precellys 24 (Bertin Biotechnologies®, France) in 1 ml of Qiazol lysis reagent (Qiagen®) on a CK28 bead tube (Bertin Biotechnologies®, France). After the addition of 200 μl of chloroform p.a. (Merck®, Darmstad, Germany), the samples were vortexed and left for 15 min before the phases were separated by centrifugation at 12,000 g for 15 min at 4 °C (Centrifuge 5415 R, Eppendorf AG, Hamburg®). The aqueous phase (RNA) was precipitated with 500 μl of isopropanol and centrifuged at 12,000 g for 10 min at 4 °C. The pellet was resuspended in 1 ml of 75% ethanol, vortexed and centrifuged at 10,500 g for 5 min at 4 °C. The pellet was subsequently dissolved in 50 μl of DEPC-treated H_2O (Invitrogen®). Total RNA quantification was performed on a Nanodrop spectrophotometer (ND-100, Thermo Fisher Scientific Inc.®, Waltham, MA), after which the samples were stored at −80 °C until analysis.

2.8. Reverse transcription-polymerase chain reaction (RT-PCR)

For the total RNA analysis, the samples were treated with RNase-free DNase (Promega®) according to the manufacturer's instructions. The cDNA was synthetized from 4 μg of total RNA, and then, 2 μg of oligo(dT) (Invitrogen®), 8 μl of 5× FS buffer (Invitrogen®), 2 μl of 10 mM dNTP, 2 μl of 0.1 M DTT (Invitrogen®), 2 μl of 40 U/μl RNAseOUT (Invitrogen®), and 2 μl of 200 U/μl M-MLV (Invitrogen®) were added. At a final volume of 40 μl, the mix was incubated at 20 °C for 10 min, at 42 °C for 45 min and then at 95 °C for 5 min.

Real-time PCR was performed for the Fibronectin 1 gene and the GAPDH gene using a SYBR Green PCR Master Mix (Applied Biosystems®, Foster City, California, USA) and a TAQMAN system. The forward and reverse primers for Fibronectin 1 (NCBI Reference Sequence: Nm_010233.1) were designed from the coding regions of the DNA sequences that were obtained from www.ncbi.nlm.nih.gov. The sequences of the primers that were used for the amplification of fibronectin 1 mRNA were as follows: (sense) 5′-CCAGGGTGTGAGCCGGACAAC-3′ and (antisense) 5′-CGAACTGTGGGTCCCCTCGC-3′. The primers used for the internal control GAPDH (*Glyceraldehyde 3-phosphate dehydrogenase*) mRNA were obtained from Applied Biosystems (Mm999 99915_g1). The amplification was performed by real-time PCR (7300 System, Applied Biosystems®) as follows: 50 °C for 2 min, 95 °C for 10 min, and then 40 cycles of 95 °C for 15 s and 60 °C for 1 min.

The statistical analysis of the quantitative RT-PCR results was performed using the ΔCt value ($Ct_{gene\ of\ interest} - Ct_{GAPDH}$). The relative gene expression was calculated with the ΔΔCt methods ($\Delta Ct_{sample} - \Delta Ct_{GAPDH}$) using the normal group as a calibrator for the comparison of every unknown sample gene expression level. The conversion between ΔΔCt and the relative gene expression levels is fold change = $2^{-\Delta\Delta Ct}$.

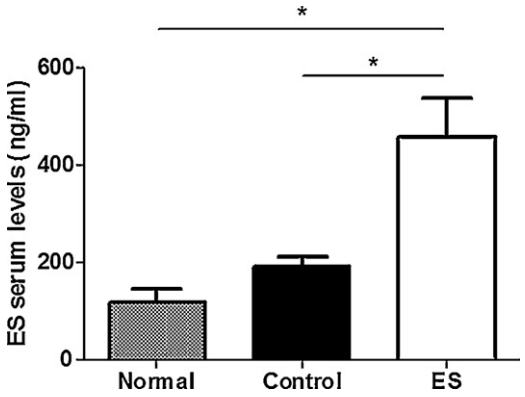

Fig. 1. Orthotopic metastatic animal model of RCC. The ES serum levels of normal and experimental groups are indicated (normal *vs* ES-treated group and control *vs* ES-treated group, $^*P < 0.05$ by ANOVA).

2.9. Statistical analysis

Statistical analysis were performed using a one-way ANOVA followed by Bonferroni's test (parametric analysis) using GraphPad prism version 5.0 for Windows® (GraphPad® Software, San Diego, CA, USA, http://www.graphpad.com). Single comparisons of the mean values were performed by Student's *t*-test. A probability (*P*) value of less than 0.05 was considered to be statistically significant. The results represent the mean ± SEM as indicated.

3. Results

At the end of the experiments, the animals were euthanized, and the levels of endogenous ES in the normal, control and ES-treated groups were measured. As shown in Fig. 1, the subcutaneous inoculation of the NIH/3T3-LendSN-clone 3 cells resulted in a significant increase of circulating ES in the ES-treated animals ($P < 0.05$).

The expression of FN was assessed using RT-PCR, immunofluorescence and western blotting. The RT-PCR analysis showed that there was a 2.0-fold decrease in FN in response to ES gene therapy (control *vs* treated group, $P < 0.001$) (Fig. 2).

The immunofluorescence data revealed that in normal lung tissues, there was no positive staining of FN (Fig. 3A). However, in metastatic lungs, a pattern of FN staining was observed with negative tumor cells and positive stroma around the tumor nodules. The metastatic lung tissues of the control group showed

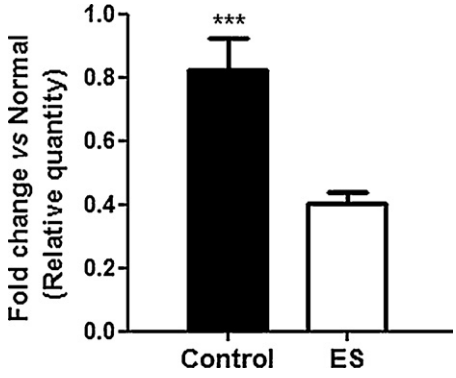

Fig. 2. The expression of the FN gene in metastatic lungs was examined using real-time PCR. The real-time PCR results were described as a fold increase relative to normal lungs following normalization against a housekeeping gene. ES treatment led to a 2.05-fold decrease in FN expression (control *vs* ES-treated, $^{***}P < 0.001$ by Student's *t*-test).

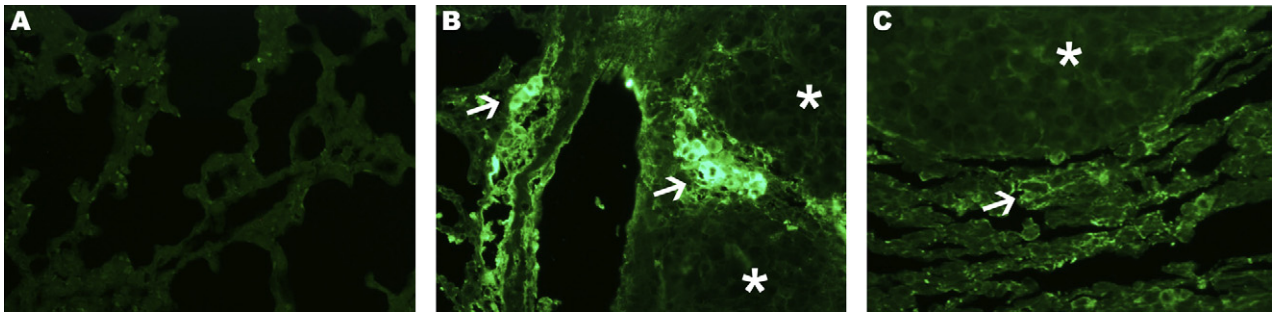

Fig. 3. Representative images of FN immunofluorescence staining in the lungs of mice from each experimental group. A. The immunofluorescence staining pattern of normal pulmonary parenchyma is shown. B. Intensive FN labeling can be observed at the periphery of the tumor nodules in the control group. C. FN staining decreased markedly after ES treatment. The asterisk indicates the metastatic nodule, and the arrow indicates FN-positive staining. Original magnification (20×).

strong, positive FN staining surrounding the nodule (Fig. 3B). As shown in Fig. 3C, ES treatment resulted in a significant reduction of FN staining.

Western blotting was performed for six tumor samples as a complementary test to evaluate the FN expression levels. All of the samples showed a band at approximately 220 kDa (Fig. 4A). The densitometric quantification of the immunoblot band data corroborated the immunofluorescence findings. In the lungs of the control group, an increase in FN by approximately 35% (control *vs* normal group; $P < 0.05$) was observed (Fig. 4B). In contrast, the concentration of FN was markedly decreased by approximately 80% in the ES-treated group (control *vs* ES-treated group; $P < 0.001$) (Fig. 4B).

4. Discussion

The tumor environment is a complex system comprising many types of cells, secreted soluble factors and non-cellular solid material. The non-cellular microenvironment is composed of extracellular matrix (ECM) proteins, including FN, laminin, collagen, osteopontin, proteoglycans, and glycosaminoglycans [26]. FN is up-regulated in different types of malignant tumors, including RCC [13,17,27–29].

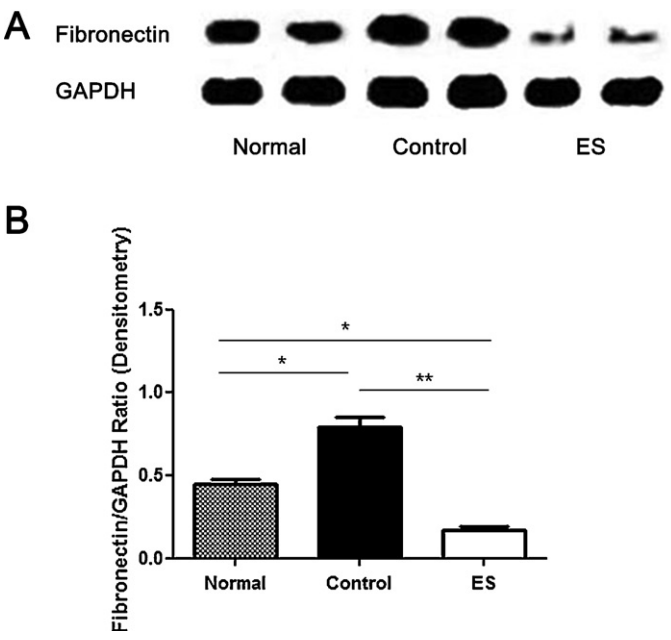

Fig. 4. Western blot analysis of FN in lung tissue samples of the normal, control and ES-treated groups. A. Lung tissue samples were randomly taken from each group and analyzed for FN protein levels by immunoblotting. The membrane was stripped and reprobed with GAPDH as a loading control. B. A significant increase in FN levels was observed in the control group (normal *vs* control, $^{*}P < 0.05$). In the lungs of the ES-treated group, the FN expression decreased dramatically (normal *vs* ES-treated, $^{*}P < 0.05$; control *vs* ES-treated, $^{**}P < 0.01$). The data are presented as the mean ± SEM and analyzed by an ANOVA test.

In this study, we demonstrated that FN is significantly increased in the lungs of the mRCC animal model. The up-regulation of FN expression has also been observed in human RCC. An *in vitro* study conducted by Brenner and collaborators demonstrated that various compounds of the extracellular matrix, especially FN, stimulate the migration of renal carcinoma cells. It has also been demonstrated that FN promotes endothelial cell survival, growth and migration, and thus, FN has a pro-angiogenic effect [30]. Waalkes and collaborators analyzed FN 1 expression in 212 renal tumor samples and found that the FN 1 mRNA expression levels were significantly higher in RCC compared to normal renal tissue and oncocytomas. In addition, elevated plasma levels of cFN were detected in patients suffering from localized and metastatic RCC [13].

It has been reported that the synthesis and deposition of FN depends on the characteristics of the tumor cells [27]. Our immunofluorescence findings showed that FN-positive staining was not detected in the tumor cells or in the adjacent normal tissues but was only in the renal parenchyma cells around the nodules. This finding suggests that the production of FN may be induced by tumor-specific growth factors.

ES treatment led to markedly reduced FN staining in the metastatic nodules. This is in agreement with the mechanism of action and the signaling induced by ES that was described by Sudhakar et al. [30]. The authors demonstrated that human ES competes with FN to bind $\alpha_5\beta_1$ integrin, which affects the survival of endothelial cells. Our data are also corroborated by the findings of Jens van Wijngaarden and collaborators (2004) [31]. In that study, a human xenograft mouse model was used, and intratumoral injection of ES caused a reduction of FN mRNA in the heterotopic implanted human renal cell carcinomas in nude mice.

In the present study, the decrease in FN protein expression was also demonstrated by western blot analysis, corroborating the hypothesis that FN expression is down-regulated by the continuous release of recombinant ES from the NIH/3T3-LendSN cells.

In conclusion, FN expression is increased in mRCC, indicating a possible role for FN in RCC progression. Our data demonstrate that sustained expression of ES led to the down-regulation of FN expression.

Disclosure of interest

The authors declare that they have no conflicts of interest concerning this article.

Acknowledgements

This study was supported by FAPESP (Process number: 2010/18969-0 and Process number: 2009/12518-9).

References

[1] Sacco E, Pinto F, Totaro A, D'Addessi A, Racioppi M, et al. Imaging of renal cell carcinoma: state of the art and recent advances. Urol Int 2011;86:125–39.
[2] Ruys AT, Tanis PJ, Iris ND, et al. Surgical treatment of renal cell cancer liver metastases: a population-based study. Ann Surg Oncol 2011;18:1932–8.
[3] Chintalapudi MR, Markiewicz M, Kose N, et al. Cyr61/CCN1 and CTGF/CCN2 mediate the pro-angiogenic activity of VHL mutant renal carcinoma cells. Carcinogenesis 2008;29:696–703.
[4] Finley DS, Pantuck AJ, Belldegrun AS. Tumor biology and prognostic factors in renal cell carcinoma. Oncologist 2011;16:4–13.
[5] Jacobcon J, Rasmuson T, Grankvist K, et al. Vascular endothelial growth factor as prognostic factor in renal cell carcinoma. J Urol 2000;163:343–7.
[6] Van der Veldt AAM, Meijerink MR, van den Eertwegh AJM, et al. Targeted therapies in renal cell cancer: recent developments in imaging. Target Oncol 2010;5:95–112.
[7] Atkins MB. Interleukin-2: clinical applications. Semin Oncol 2002;29:12–7.
[8] Paule B, Bastien L, Deslandes E, et al. Soluble isoforms of vascular endothelial growth factor are predictors of response to sunitinib in metastatic renal cell carcinomas. PLoS One 2010;5:e10715.
[9] Chowdhury S, Larkin JM, Gore ME. Recent advances in the treatment of renal cell carcinoma and the role of targeted therapies. Eur J Cancer 2008;44:2152–61.
[10] Di Lorenzo G, Autorino R, Sternberg CN. Metastatic renal cell carcinoma: recent advances in the targeted therapy era. Eur Urol 2009;56:959–71.
[11] Wickström SA, Alitalo K, Keski-Oja J. Endostatin associates with integrin alpha5beta1 and caveolin-1, and activates Src via a tyrosyl phosphatase-dependent pathway in human endothelial cells. Cancer Res 2002;62:5580–9.
[12] Desgrosellier JS, Cheresh DA. Integrins in cancer: biological implications and therapeutic opportunities. Nat Rev Cancer 2010;10:9–22.
[13] Hegele A, Hofmann R, Kosche B, et al. Evaluation of cellular fibronectin plasma levels as a useful staging tool in different stages of transitional cell carcinoma of the bladder and renal cell carcinoma. Biomark Insights 2007;2:1–7.
[14] Kriegsmann J, Berndt A, Hansen T, et al. Expression of fibronectin splice variants and oncofetal glycosylated fibronectin in the synovial membranes of patients with rheumatoid arthritis and osteoarthritis. Rheumatol Int 2004;24:25–33.
[15] Malik G, Knowles LM, Dhir R, et al. Plasma fibronectin promotes lung metastasis by contributions to fibrin clots and tumor cell invasion. Cancer Res 2010;70:4327–34.
[16] Waalkes S, Atschekzei F, Kramer MW, et al. Fibronectin 1 mRNA expression correlates with advanced disease in renal cancer. BMC Cancer 2010;10:503.
[17] Brenner KA, Corbett SA, Schwarzbauer JE. Regulation of fibronectin matrix assembly by activated Ras in transformed cells. Oncogene 2000;19:3156–63.
[18] Xie L, Duncan MB, Pahler J, et al. Counterbalancing angiogenic regulatory factors control the rate of cancer progression and survival in a stage-specific manner. Proc Natl Acad Sci U S A 2011;108:9939–44.
[19] Coutinho EL, Andrade LNS, Chammas R, et al. Anti-tumor vector of endostatin mediated by retroviral gene transfer in mice bearing renal cell carcinoma. FASEB J 2007;21:3153–61.
[20] Rocha FG, Chaves KC, Chammas R, et al. Endostatin gene therapy enhances the efficacy of IL-2 in suppressing metastatic renal cell carcinoma in mice. Cancer Immunol Immunother 2010;59:1357–65.
[21] Rocha FG, Chaves KC, Gomes CZ, Campanharo CB, et al. Erythrocyte protoporphyrin fluorescence as a biomarker for monitoring antiangiogenic cancer therapy. J Fluoresc 2010;20:1225–31.
[22] Rocha FG, Calvo FB, Chaves KC, et al. Endostatin- and interleukin-2-expressing retroviral bicistronic vector for gene therapy of metastatic renal cell carcinoma. J Gene Med 2011;13:148–57.
[23] Digtyar AV, Pozdnyakova NV, Feldman NB, et al. Endostatin: current concepts about its biological role and mechanisms of action. Biochemistry (Mosc) 2007;72:235–46.
[24] Rehn M, Veikkola T, Kukk-Valdre E, et al. Interaction of endostatin with integrins implicated in angiogenesis. Proc Natl Acad Sci U S A 2001;98:1024–9.
[25] Wickström SA, Veikkola T, Rehn M, Pihlajaniemi T, et al. Endostatin-induced modulation of plasminogen activation with concomitant loss of focal adhesions and actin stress fibers in cultured human endothelial cells. Cancer Res 2001;61:6511–6.
[26] Fan F, Schimming A, Jaeger D, et al. Targeting the tumor microenvironment: focus on angiogenesis. J Oncol 2011;2012:1–16.
[27] Zhang J, Zhi H, Zhou C, et al. Up-regulation of fibronectin in oesophageal squamous cell carcinoma is associated with activation of the Erk pathway. J Pathol 2005;207:402–9.
[28] Han S, Khuri FR, Roman J. Fibronectin stimulates non–small cell lung carcinoma cell growth through activation of Akt/mammalian target of rapamycin/S6 kinase and inactivation of LKB1/AMP-activated protein kinase signal pathways. Cancer Res 2006;66:315–23.
[29] Murata J, Saiki I, Yoneda J, et al. Differences in chemotaxis to fibronectin in weakly and highly metastatic tumor cells. Jpn J Cancer Res 1992;83:1327–33.
[30] Sudhakar A, Sugimoto H, Yang C, et al. Human tumstatin and human endostatin exhibit distinct antiangiogenic activities mediated by alpha v beta 3 and alpha 5 beta 1 integrins. Proc Natl Acad Sci U S A 2003;100:4766–71.
[31] van Wijngaarden J, de Rooij K, van Beek E, et al. Identification of differentially expressed genes in a renal cell carcinoma tumor model after endostatin-treatment. Lab Invest 2004;84:1472–83.